

Direct visualization of Bcl-2 family protein interactions using live cell fluorescent protein redistribution assays

C Wong^{1,4}, DJ Anderson^{1,4}, EF Lee^{2,3}, WD Fairlie^{2,3} and MJC Ludlam^{*1}

Bcl-2 family proteins have important roles in tumor initiation, progression and resistance to therapy. Pro-survival Bcl-2 proteins are regulated by their interactions with pro-death BH3-only proteins making these protein–protein interactions attractive therapeutic targets. Although these interactions have been extensively characterized biochemically, there is a paucity of tools to assess these interactions in cells. Here, we address this limitation by developing quantitative, high throughput microscopy assays to characterize Bcl-2 and BH3-only protein interactions in live cells. We use fluorescent proteins to label the interacting proteins of interest, enabling visualization and quantification of their mitochondria-localized interactions. Using tool compounds, we demonstrate the suitability of our assays to characterize the cellular activity of putative therapeutic molecules that target the interaction between pro-survival Bcl-2 and pro-death BH3-only proteins. In addition to the relevance of our assays for drug discovery, we anticipate that our work will contribute to an improved understanding of the mechanisms that regulate these important protein–protein interactions within the cell.

Cell Death and Disease (2012) 3, e288; doi:10.1038/cddis.2012.28; published online 29 March 2012

Subject Category: Cancer

The intrinsic apoptotic cell death pathway is mediated by three factions of the Bcl-2 protein family. The pro-death BH3-only proteins, which include Bim, Puma, Noxa, Bad, Bid and several others engage pro-survival proteins, Bcl-2, Bcl-x_L, Bcl-w, Mcl-1 and A1 thereby blocking pro-survival function.^{1,2} The third sub-family comprises the multi-domain pro-apoptotic proteins Bax and Bak, which mediate mitochondrial outer membrane permeabilization leading to cytochrome *c* release, caspase cascade activation and ultimately cell death.^{3,4} Overexpression of Bcl-2 and its pro-survival relatives has been reported in many cancer types and typically correlates with poor survival and disease progression, as well as resistance to chemotherapeutics.^{5,6} Consequently, pro-survival Bcl-2 proteins are appealing drug targets.^{7,8}

Inhibition of the interactions between the Bcl-2 pro-survival proteins and their BH3-only counterparts is a popular therapeutic approach and several of the resulting BH3 mimetic inhibitors have entered clinical trials.^{8,9} ABT-737 is a BH3 mimetic, small molecule inhibitor of BH3-only interactions with Bcl-2, Bcl-x_L and Bcl-w that exemplifies this approach.¹⁰ Although tools such as nuclear magnetic resonance-based screening along with fluorescence polarization and time resolved fluorescence resonance energy transfer measurements have proven invaluable for identification and characterization of the selectivity and potency of such inhibitors in a biochemical setting,^{10,11} there is a lack of tools to evaluate the activity of such compounds in cells. Therefore, cellular validation of such compounds typically relies on detection of downstream read-outs such as cytochrome

c release or cell viability.^{10,11} However, these assays are unable to verify biochemically determined specificities and may thus prioritize irrelevant compounds that cause death by off-target mechanisms.

Given the considerable role of Bcl-2 family proteins in tumorigenesis and the resulting enthusiasm to target them therapeutically, understanding the interactions and dynamics of the Bcl-2 family members in the cellular context and the development of tools to do so remain important challenges. Although Bcl-2 family interactions have been the subject of systematic *in vitro* studies that characterized the selectivity of these interactions using BH3 peptides,^{12–14} no comparable characterization of the behavior of full-length proteins in intact cells has been reported. To address this, we have developed microscopy-based assays that directly measure the interactions of Bcl-2 pro-survival with pro-apoptotic BH3-only proteins in live cells, preserving the interacting proteins in the mitochondrial membrane environment that is known to be critical for their activity.¹⁵ These assays are based on differential fluorescent protein tagging of the proteins of interest, allowing us to visualize their colocalization at the mitochondria. Treatment of cells expressing these proteins with an inhibitor, such as ABT-737, caused relocalization of the BH3-only protein to the cytoplasm and thus provides a sensitive read-out for disruption of the protein–protein interaction of interest that is compatible with adaptation to a throughput relevant for drug screening.¹⁶

¹Department of Research Oncology, Genentech, Inc., 1 DNA Way, South San Francisco, CA 94080, USA; ²The Walter and Eliza Hall Institute of Medical Research, 1G Royal Pde, Parkville, Victoria 3052, Australia and ³Department of Medical Biology, The University of Melbourne, Parkville, Victoria, Australia

*Corresponding author: M Ludlam, Department of Research Oncology, Genentech, Inc., 1 DNA Way, South San Francisco, CA 94080, USA. Tel: 1 650 225 1299; Fax: 1 650 742 1580; E-mail: ludlam.mary@gene.com or maryludlam@gmail.com

⁴These authors contributed equally to this work.

Keywords: apoptosis; Bcl-2 family; cancer; microscopy; drug screening

Abbreviations: ER, endoplasmic reticulum; IRES, internal ribosome entry site; DMSO, dimethyl sulfoxide; FBS, fetal bovine serum

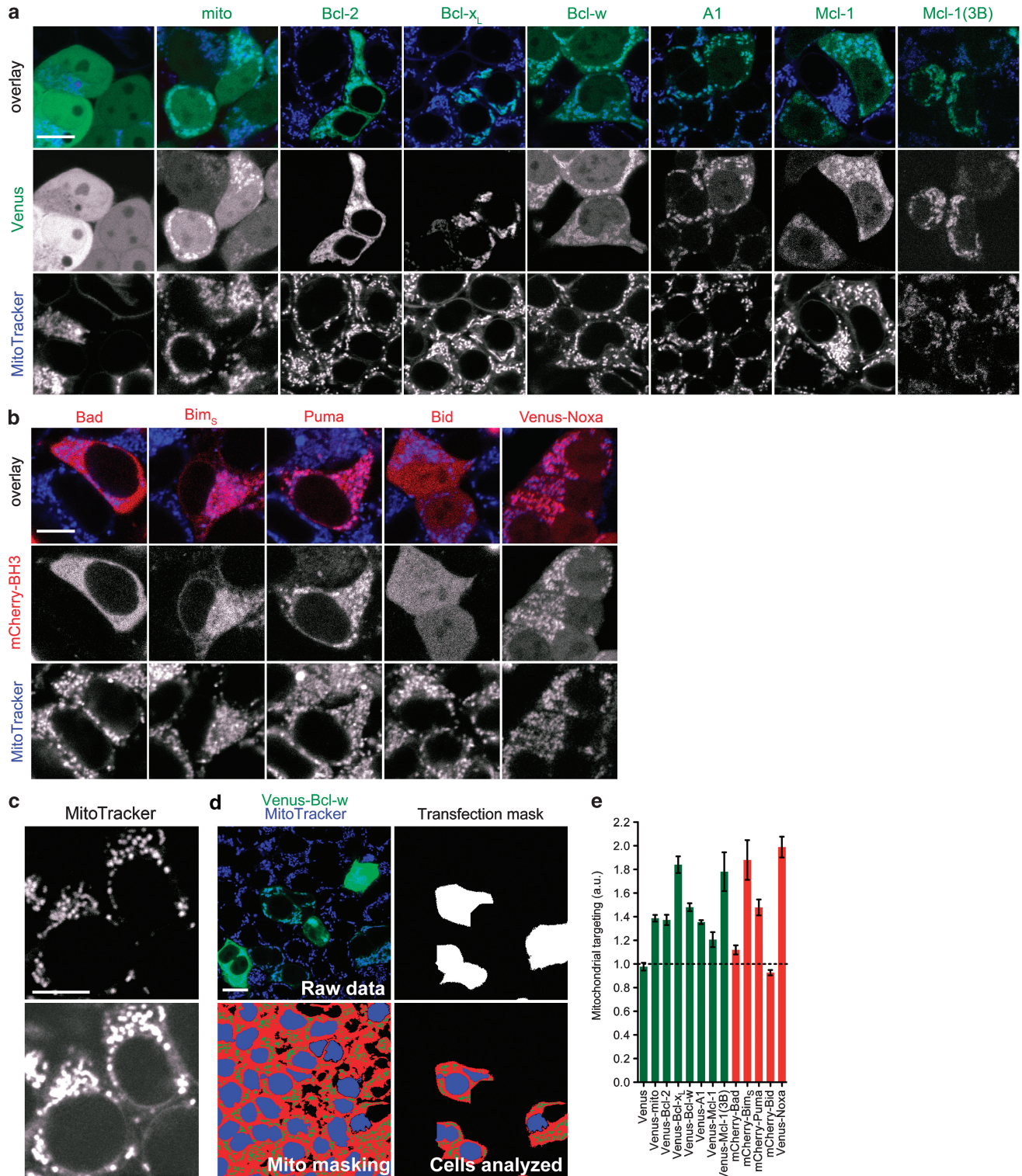
Received 22.11.11; revised 11.1.12; accepted 31.1.12; Edited by D Bano

Results

Quantitative localization of Bcl-2 super-family proteins in live cells. To first confirm our ability to visualize Bcl-2 super-family proteins in live cells, we generated fluorescent protein fusions to the Bcl-2 pro-survival and BH3-only sub-family members and examined their localization in transiently

transfected HEK293T cells. Because all Bcl-2 pro-survival proteins and many BH3-only proteins contain C-terminal membrane targeting domains,¹⁷ we labeled the proteins of interest at their N-terminus.

Venus fluorescent protein fusions to the N-terminus of the pro-survival proteins Bcl-2, Bcl-x_L, Bcl-w, Mcl-1 and A1 all localized to the mitochondria as determined by colocalization



with MitoTracker Deep Red dye (Life Technologies, Carlsbad, CA, USA), which stains mitochondria in live cells (Figure 1a). Consistent with previous reports,^{18,19} we showed that Bcl-2 also localized to the endoplasmic reticulum (ER), as determined by cotransfection of mCherry-Bcl-2 with eCFP-calreticulin (Supplementary Figure 1a). As previously reported,²⁰ Mcl-1 showed proportionately weak mitochondrial localization, which we anticipated would compromise our ability to develop a quantitative Mcl-1-specific component of the assay. We therefore generated an Mcl-1 mutant with increased mitochondrial targeting by replacing three residues in its C-terminal tail region with basic residues (Mcl-1(3B)) (Figure 1a and Supplementary Table 1).²¹ As expected, our positive control, Venus-mito (subunit VIII of cytochrome *c* oxidase), targets to the mitochondrial lumen with partial cytoplasmic localization and our negative control, Venus protein, is cytoplasmic and not observably absent from the mitochondria (Figure 1a).

The mCherry-BH3-only protein constructs targeted to the mitochondria and ER in the case of Bim_S and Puma, and the cytoplasm in the case of Bad and Bid (Figure 1b and Supplementary Figure 1a). As mCherry-Noxa formed puncta that did not localize to the mitochondria and that were indicative of aggregates, (Supplementary Figure 1b), we generated a Venus-Noxa construct and verified its localization to the mitochondria (Figure 1b).

To confirm that the localization of our Bcl-2 family fluorescent protein reporters parallels that of endogenous proteins, we conducted immunofluorescence in untransfected HEK293T cells. Localization of each fluorescent fusion protein was similar to the endogenous protein localization (Supplementary Figure 2). Combined with our observations above, these data confirm that N-terminally fluorescent protein-tagged Bcl-2 pro-survival and BH3-only proteins localize correctly and are an appropriate basis on which to further develop our assay.

We extended the above qualitative evaluation of our fluorescent fusion proteins by developing an automated method to quantify their mitochondrial targeting. We used the differential intensities of MitoTracker dye in the mitochondria, cytoplasm and nucleus (Figure 1c) to segment these compartments using iterative threshold combined with shape- and size-based object detection written in MATLAB (Figure 1d; Mito masking). As we noted that our constructs formed large aggregates in cells expressing high levels of fluorescent protein, we used intensity threshold to identify these cells and the associated cytoplasm mask to exclude these cells from our analysis (Figure 1d; Transfection mask). Combined, these approaches enable automated measurement of fluorescence intensity in the mitochondria and cytoplasm of transfected cells within a defined range of

expression levels. When we calculated the degree of mitochondrial targeting for each Bcl-2 family member using the ratio of mitochondrial to cytoplasmic fluorescence intensity, we determined that proteins that did not visibly localize to the mitochondria, such as Venus, Bad and Bid, had a ratio < 1.1, whereas proteins with at least partial mitochondrial localization had ratios in excess of 1.2 (Figure 1e).

Relocalization of BH3-only proteins by their Bcl-2 pro-survival counterparts can be visualized and quantified in live cells.

Having established the baseline amount of mitochondrial targeting for each of our individual constructs, we next investigated the behavior of cotransfected Bcl-2 pro-survival and BH3-only protein pairs. We hypothesized that a cytoplasmic BH3-only protein, such as Bad, would target to the mitochondria upon coexpression of its pro-survival Bcl-2 family binding partners, Bcl-2, Bcl-x_L and Bcl-w but not Mcl-1 or A1 (Figure 2a).¹² As expected, we only observed recruitment of mCherry-Bad to the mitochondria when it was cotransfected with Venus-Bcl-2, Bcl-x_L and Bcl-w with additional targeting to the ER in the case of Bcl-2 (Figure 2b and c). These data suggest that the targeting of Bad to the mitochondria can be used as a surrogate read-out of binding to pro-survival proteins.

In principle, the approach described above could be used to investigate the interactions between all pro-apoptotic proteins and Bcl-2 family members, however, the mitochondrial localization of Bim_S, Puma and Noxa precludes this. We therefore generated mutants of these proteins that we hypothesized would localize to the cytosol and then relocate to the mitochondria upon cotransfection with their Bcl-2 pro-survival partners (Supplementary Table 1). As Bim_S, Puma and Noxa are associated with membranes such as those of the mitochondria via a hydrophobic C-terminus for Bim_S,²² and a C-terminal membrane targeting domain for Puma²³ and Noxa^{24,25} we truncated these regions from the C-terminus of each protein (denoted by ΔC), thus abolishing membrane targeting (Figures 2d and e). Unlike the other BH3-only proteins, full length Bid is inactive until cleaved by caspase 8, to give rise to truncated Bid (tBid).^{26,27} Recent studies have shown that tBid targets to the mitochondria via binding of the helix αH6 in tBid to mitochondrial cardiolipin.²⁸ To abrogate this mitochondrial targeting, we made an αH6 deletion mutant, tBidΔH6 (Figure 2j and Supplementary Figure 3c). As none of these constructs showed accumulation at the mitochondria when transfected alone, we conclude that binding of these BH3-only mutants to endogenous Bcl-2 family proteins is negligible. Next, we tested the ability of pro-survival Bcl-2 family proteins to recruit the BH3-only mutants described above by cotransfecting the relevant constructs. We observed

Figure 1 Quantitative assessment of Bcl-2 family protein localization to the mitochondria in live cells. (a and b) HEK293T cells were transfected with fluorescent protein fusions to Bcl-2 family members, stained with MitoTracker dye (blue) and visualized live using confocal microscopy. (a) Localization of pro-survival Venus-Bcl-2 family constructs (green). The mitochondrial targeting peptide of subunit VIII of cytochrome *c* oxidase fused to the carboxy-terminus of Venus (Venus-mito) was used as a positive control and Venus alone was used as a negative control. (b) Localization of mCherry- or Venus- (in the case of Noxa) tagged-BH3-only proteins (red). (c) Two different exposure images exemplifying the differential intensities of MitoTracker staining in the mitochondria and cytoplasm that were used as the basis for image analysis depicted in d. (d) Image analysis protocol used to quantify mitochondrial targeting of fluorescent fusion proteins. MitoTracker staining (blue in raw data) was used to mask the cytoplasm, nucleus and mitochondria (red, blue and green, respectively, in Mito masking). Cells within an appropriate range of expression levels for quantification were identified (transfection mask) and fluorescence intensities were measured in these cells (cells analyzed). (e) Measurement of mitochondrial targeting for each pro-survival (green) and pro-death (red) Bcl-2 super-family fluorescent construct. Mitochondrial targeting is denoted by the ratio of mitochondrial to cytoplasmic fluorescence intensity measured according to the protocol described in d. A ratio of one represents no detectable mitochondrial targeting. Scale bars 10 μm

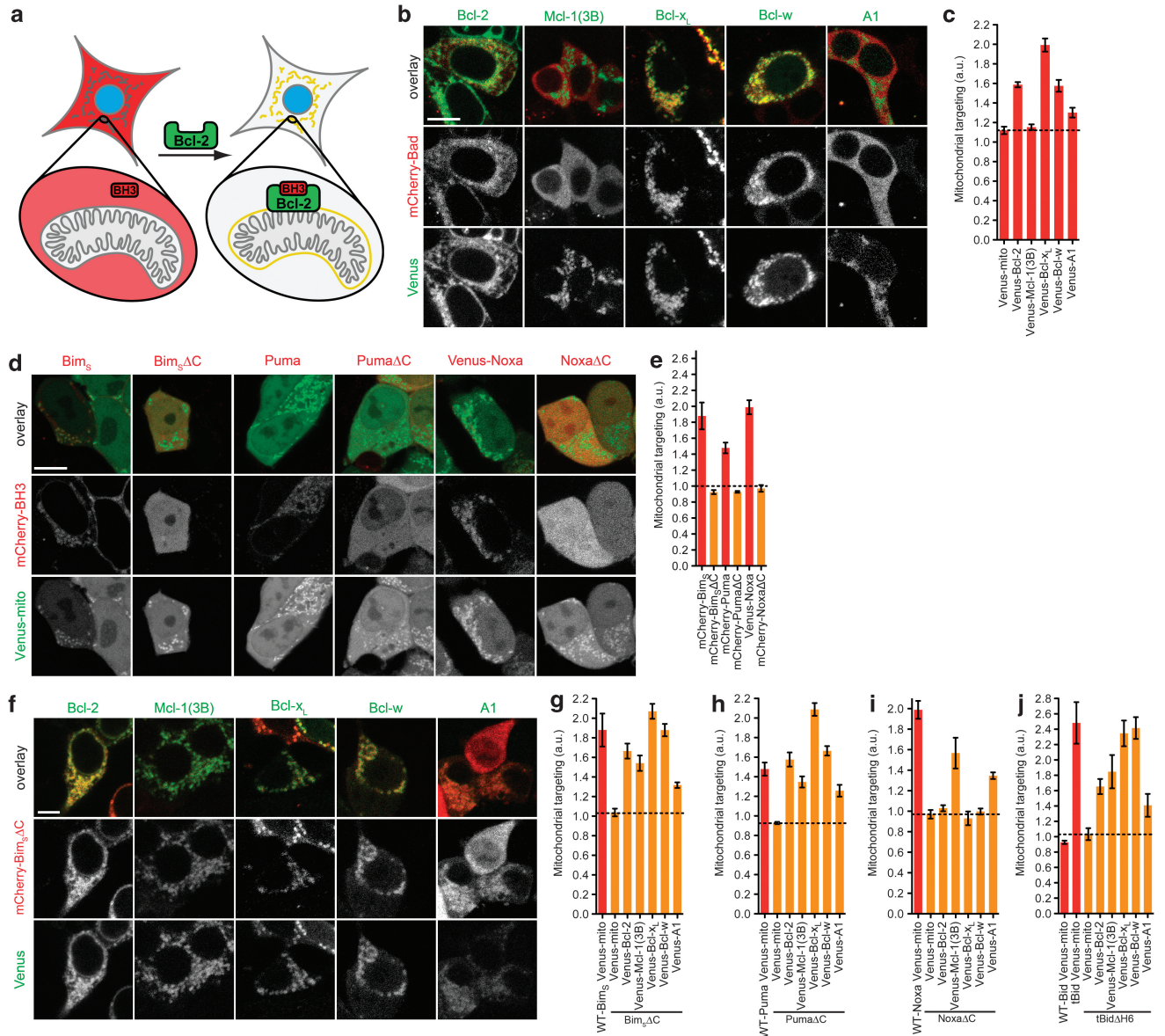


Figure 2 Pro-survival Bcl-2 proteins relocate their cytoplasmically localized BH3-only protein-binding partners to the mitochondria. (a) Assay schematic in which a cytoplasmic BH3-only protein (red) is recruited to the mitochondria when coexpressed with a mitochondrially localized Bcl-2-binding partner protein (green) resulting in colocalization (yellow). (b) Localization of mCherry-Bad (red) when cotransfected with Venus-tagged pro-survival Bcl-2 family members (green) in live HEK293T cells. (c) Measurement of mitochondrial targeting of mCherry-Bad when cotransfected with Venus tagged pro-survival family members or a Venus-mito control. (d) Mitochondrially localized BH3-only proteins were truncated to remove the C-terminal membrane-targeting domain (ΔC). mCherry-fusions to the truncation mutants (red) were cotransfected with Venus-Mito (green) and their localization was compared with their wild-type counterparts. (e) Measurement of mitochondrial targeting of each mCherry tagged wild-type (red) and ΔC (orange) BH3-only protein shown in d. (f) Localization of mCherry-Bim ΔC (red) when cotransfected with Venus-Bcl-2 pro-survival proteins (green) in live HEK293T cells. (g–j) Measurement of the relocalization of cytoplasmically localized mCherry tagged BH3-only mutants (orange) to the mitochondria when cotransfected with their Venus tagged pro-survival binding partners. Behavior of wild-type mCherry tagged BH3-only proteins is shown as a control (red): (g) Bim ΔC , (h) Puma ΔC , (i) Noxa ΔC , (j) tBid $\Delta H6$. Scale bars 10 μm

that Bim ΔC , Puma and tBid mutants relocalized to the mitochondria in the presence of Bcl-2, Bcl-x $_L$, Bcl-w, A1 and Mcl-1(3B) whereas Noxa ΔC only relocalizes with Mcl-1(3B) and A1. (Figures 2d–j, Supplementary Figures 3a–c and Supplementary Table 2), paralleling the observations of previously published biochemical studies on the selectivity profiles of these BH3-only proteins.^{12–14}

Taken together, these data indicate that our fluorescently tagged pro-survival Bcl-2 constructs are capable of

relocalizing fluorescently tagged BH3-only proteins with which they interact. Furthermore deletion of membrane targeting domains from BH3-only proteins that are normally constitutively localized to the mitochondria and ER abolishes their subcellular targeting but not their ability to interact with their pro-survival counterparts, corroborating earlier work that has shown that binding specificity is determined solely by the BH3-binding sequence.^{12–14,29} Combined, our

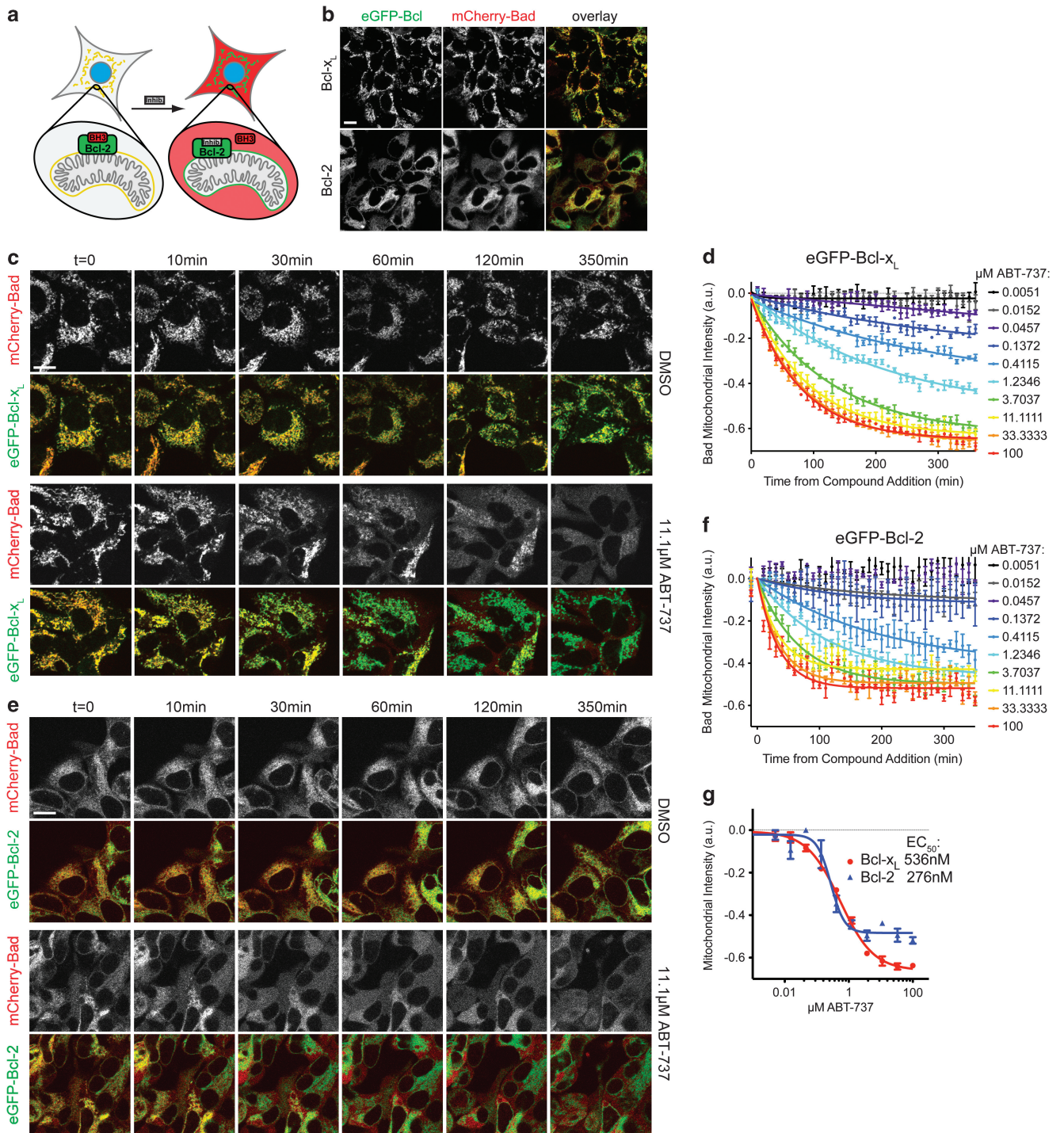


Figure 3 Compound-mediated disruption of Bcl-2 family protein–protein interactions can be measured in live cells. (a) Schematic showing displacement of a BH3-only protein (red) from its mitochondrially localized Bcl-2-binding partner (green) to the cytoplasm by a BH3-mimetic inhibitor (gray). (b) Confocal images of live stable, inducible T-REx-293 cells expressing a bicistronic construct of mCherry-Bad (red) with either eGFP-Bcl-2 or eGFP-Bcl-x_L (green) 16 h after doxycycline treatment. (c) Time-lapse images of T-REx-293 eGFP-Bcl-x_L/mCherry-Bad cells treated with 1% DMSO or ABT-737 (11.1 μM). (d) Mitochondrial intensity of mCherry-Bad was measured for time-lapse series exemplified in (c). Decrease in mCherry-Bad mitochondrial intensities were calculated for a three-fold dilution series of ABT-737 (100 to 5.1 nM), normalized to DMSO control and fitted to a single exponential decay. (e) Time-lapse images of T-REx-293 eGFP-Bcl-2/mCherry-Bad cells treated with 1% DMSO or ABT-737 (11.1 μM). (f) Mitochondrial intensity of mCherry-Bad was measured for time-lapse series exemplified in (e) and quantified as in (d). (g) Interpolated mitochondrial intensities of mCherry-Bad at 350 min from (d) and (f) were fitted to a sigmoidal curve to calculate cellular EC₅₀ values of ABT-737 for Bcl-x_L and Bcl-2. Scale bars 10 μm

observations thus permit extension of our approach to all Bcl-2 pro-survival and BH3-only protein–protein interactions.

Measurement of compound-mediated disruption of Bcl-2 family protein–protein interactions in live cells. Having generated and validated a panel of constructs to investigate

Bcl-2 family protein–protein interactions in live cells, we next investigated whether our approach could be used to detect a compound-mediated disruption of the interaction between Bcl-2 pro-survival and BH3-only proteins (Figure 3a). We anticipated that variable expression levels of protein fusions from cell to cell would limit our ability to precisely measure BH3-only protein displacement following compound treatment and that constitutive BH3-only protein overexpression would compromise cell viability. We therefore generated dual labeled stable cell lines with approximately balanced expression of the pro-survival Bcl-2 and pro-death BH3-only constructs under inducible control as previously described.¹⁶

Using this method, we generated inducible T-REx-293 stable cell lines (Invitrogen, Carlsbad, CA, USA) coexpressing mCherry-Bad and eGFP-Bcl-x_L or eGFP-Bcl-2 separated by an internal ribosome entry site (IRES). eGFP was used as a fusion partner in place of Venus to improve spectral separation allowing for increased image acquisition throughput. Upon doxycycline treatment of these cell lines, we observed low-level induction of the expression of both fluorescent fusions (Figure 3b). As expected, mCherry-Bad colocalized with eGFP-Bcl-x_L at the mitochondria and colocalized with eGFP-Bcl-2 at both the mitochondria and ER. Importantly, mitochondrial morphology appeared unperturbed when compared with wild-type cells stained with MitoTracker dye (Figures 3b and 1c).

We treated our eGFP-Bcl-x_L/mCherry-Bad and eGFP-Bcl-2/mCherry-Bad stable cell lines with ABT-737 and, consistent with previous reports,³⁰ we observed displacement of mCherry-Bad from membrane localized eGFP-Bcl-2 and eGFP-Bcl-x_L after ABT-737 addition (Figures 3c and e and Supplementary Movie). To quantify this effect, we adapted our earlier approach to quantification by segmenting the localization of the pro-survival proteins then measuring mCherry fluorescence intensity within this region. We verified that control dimethyl sulfoxide (DMSO)-treated cells did not show a decrease in fluorescence intensity of either channel, confirming that the 6 h time-lapse acquisition did not result in appreciable photobleaching (Supplementary Figures 4a–b). Additionally, the decrease in mCherry-Bad intensity after ABT-737 treatment was not because of decreased eGFP-Bcl-x_L or eGFP-Bcl-2 protein levels as eGFP fluorescence intensity remained constant throughout the 6 h time course of the experiment (Supplementary Figure 4a). Furthermore, the decrease in mCherry-Bad protein intensity after ABT-737 treatment was not because of decreased mCherry-Bad protein levels as the average total mCherry fluorescence intensity in the acquisition fields remained constant throughout the 6 h time course of the experiment (Supplementary Figure 4b). We normalized the mCherry-Bad intensities to those measured in DMSO control treated cells and expressed them as the fold change from control treatment (Figures 3d and f). We noted that the measured intensity decrease fits to a single-phase exponential decay curve with an average F^2 value of 0.94 ± 0.04 suggesting displacement occurred via competitive binding, consistent with the paradigm that BH3 mimetics such as ABT-737 displace BH3-only proteins from the binding groove on pro-survival proteins.^{10,31} We calculated EC₅₀ values by interpolating 6 h endpoint intensities from the decay curves of mCherry-Bad and fitting them to a sigmoidal curve for the 10-point serial dilution of ABT-737

Table 1 BH3 affinity mutant peptide IC₅₀ and EC₅₀ values

	<i>In vitro</i> ^a IC ₅₀ (nM)		Cellular ^b EC ₅₀ (nM)	
	Bcl-x _L	Bcl-2	Bcl-x _L	Bcl-2
BadBH3 WT	14.0	31.0	9161.0	539.9
BadBH3 F23A	7.0	144.0	2354.0	153.5
BadBH3 F19A	29.0	2300.0	133.6	ND
BadBH3 D17A	50.0	1500.0	305.1	156.5
Bim _S L62YF69R	300.0	ND	11.8	ND

^aBH3 affinity mutant peptides measured by surface plasmon resonance.
^bBim_S-BadBH3ΔC affinity mutant stable cell lines treated with ABT-737 and measured by redistribution assay

yielding EC₅₀ doses of 536 nM and 276 nM for Bcl-x_L and Bcl-2, respectively (Figure 3g). As expected, when we added ABT-737 to our control cell line coexpressing eGFP-Mcl-1(3B) and mCherry-Bim_SΔC, which is not targeted by this BH3 mimetic, no decrease in mCherry intensity was observed in the mitochondria (Supplementary Figure 4c). These data confirm that the relocalization of Bad observed in cell lines expressing Bcl-x_L or Bcl-2 was not because of general toxicity of ABT-737.

Assay stringency can be adjusted by incorporating BH3-only protein mutants with reduced affinity for their Bcl-2 pro-survival protein-binding partners. We anticipated that the high affinity of Bad for Bcl-x_L and Bcl-2 would limit the ability of our assay to identify a diverse range of compounds capable of disrupting these interactions. We therefore considered how to configure our assay so that it would be useful for identifying compounds within an expanded range of potency while preserving their specificity for particular Bcl-2/BH3-only interactions. We hypothesized that this goal could be met by incorporating BH3-only mutants with diminished affinity for their Bcl-2 pro-survival partners, thereby reducing assay stringency.

To identify mutants within the BH3 domain of Bad that conferred varying affinities for the pro-survival proteins, we performed alanine scanning mutagenesis on a phage displayed 26-amino-acid sequence encompassing the BadBH3 domain, as described previously for BimBH3.²⁹ By measuring the affinity of each mutant for pro-survival proteins, we identified alanine substitutions including D17A, F19A and F23A that impaired binding to Bcl-x_L and/or Bcl-2. As the alanine scanning data reflected the binding of each sequence expressed on phage particles, we also determined the affinities of the isolated sequences for the pro-survival proteins using 26-mer BadBH3 synthetic peptides harboring these mutations in solution competition assays (Table 1).

We used these mutations as a basis for generating a panel of Bcl-2 and Bcl-x_L stable cell lines with a range of BH3-only binding partner affinities. We incorporated the mutations into Bim_SΔC chimeras in which the BimBH3 domain was replaced with that of Bad (resulting in Bim_S-BadBH3ΔC) (Supplementary Table 1); these chimeras have previously been shown to adopt the binding profile of the inserted BH3 domain.¹² In addition, we further expanded the range of affinities probed by this assay by incorporating a previously described³² weak-binding mutant (L62Y,F69R) of Bim_SΔC into our Bcl-x_L cell line.

The affinity mutant stable cell lines revealed visible and quantitative differences in mCherry localization (Figures 4a–d). All of the Bim_S-Bad chimeras colocalized with Bcl-x_L at the mitochondria, consistent with the relatively high *in vitro*

affinity of these mutants for Bcl-x_L (IC₅₀ ≤ 50 nM). Conversely, the Bim_S L62Y/F69R mutant with comparably low *in vitro* affinity for Bcl-x_L (IC₅₀ = 300 nM) showed higher cytoplasmic localization when compared with the Bim_S-Bad chimeras.

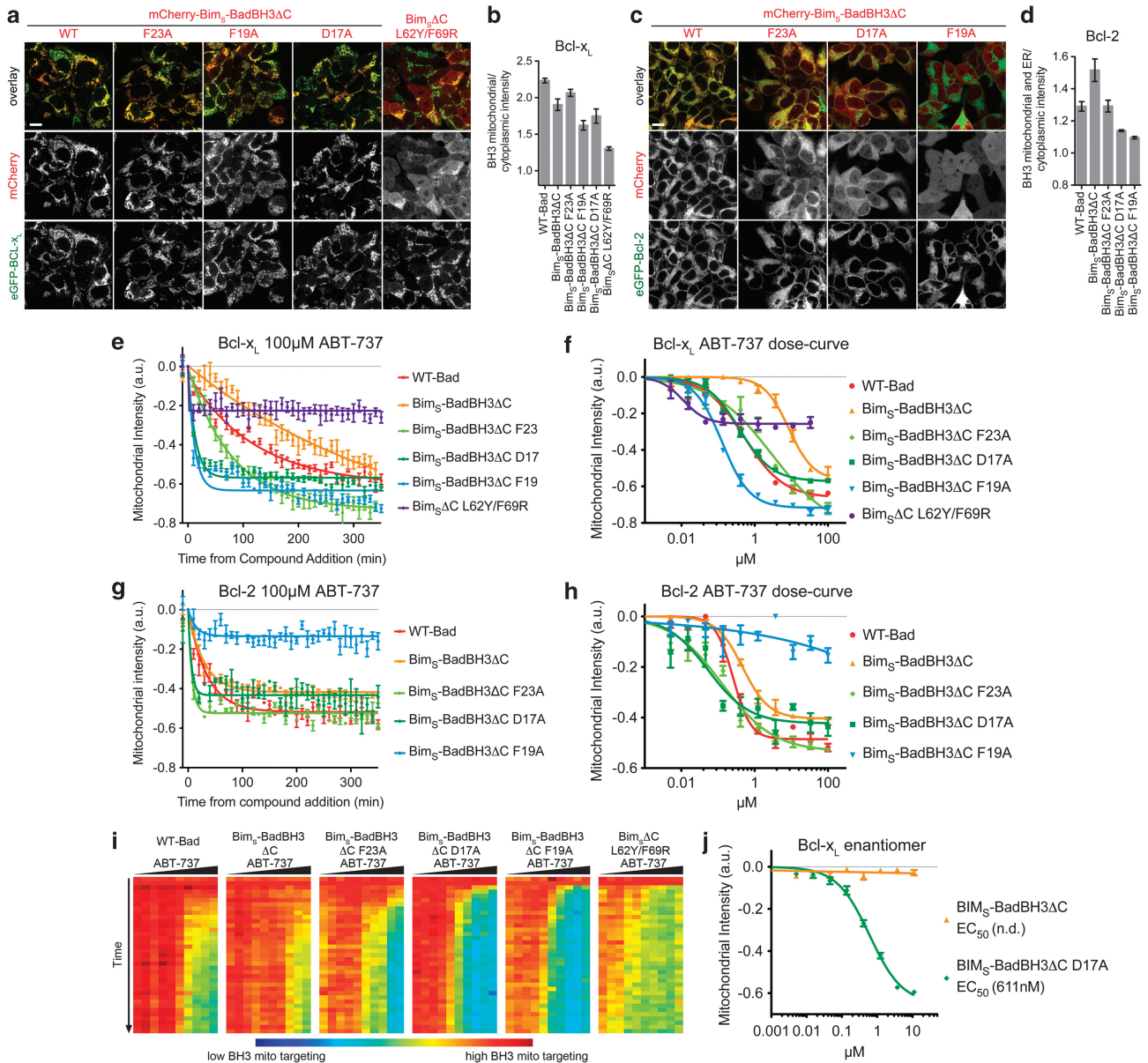


Figure 4 BH3-only affinity mutants can be used to adjust assay stringency. (a) Confocal images of live stable, inducible T-REX-293 cells expressing bicistronic constructs of mCherry-Bim_S-BadBH3ΔC affinity mutants (red, described in Supplementary Table 1) with eGFP-Bcl-x_L (green) 16 h after doxycycline induction. (b) Ratio of mitochondria to cytoplasmic mCherry-Bim_S-BadBH3ΔC intensities measured for all cell lines represented in a. (c) Confocal images of live stable, inducible T-REX-293 cells expressing bicistronic constructs of mCherry-Bim_S-BadBH3ΔC affinity mutants (red) with eGFP-Bcl-2 (green) 16 h after doxycycline induction. (d) Ratio of mitochondrial and ER to cytoplasmic mCherry-Bim_S-BadBH3ΔC intensities measured for all cell lines represented in c. (e) Mitochondrial intensity measurements of mCherry-Bim_S-BadBH3ΔC affinity mutants in response to 100 μM ABT-737 treatment of Bcl-x_L affinity mutant stable cell lines. (f) Interpolated mitochondrial intensities of mCherry-Bim_S-BadBH3ΔC affinity mutants at 350 min from Supplementary Figures 5a–e were fitted to a sigmoidal curve to calculate cellular EC₅₀ values of ABT-737 for each affinity mutant in the background of eGFP-Bcl-x_L coexpression. (g) Mitochondrial intensity measurements of mCherry-Bim_S-BadBH3ΔC affinity mutants in response to 100 μM ABT-737 treatment of Bcl-2 affinity mutant stable cell lines. (h) Interpolated mitochondrial intensities of mCherry-Bim_S-BadBH3ΔC affinity mutants at 350 min from Supplementary Figures 5f–i were fitted to a sigmoidal curve to calculate cellular EC₅₀ values of ABT-737 for each affinity mutant in the background of eGFP-Bcl-2 coexpression. (i) Heat map representation of BH3-only mitochondrial targeting in response to a dose titration of ABT-737 in all Bcl-x_L cell lines conducted as a single simultaneous experiment to exemplify throughput of redistribution assays. (j) Interpolated mitochondrial intensities of mCherry-Bim_S-BadBH3ΔC and mCherry-Bim_S-BadBH3ΔC D17A at 350 min from Supplementary Figures 5j and k were fitted to a sigmoidal curve to calculate cellular EC₅₀ values of the ABT-737 enantiomer for each affinity mutant in the background of eGFP-Bcl-x_L coexpression

Similarly, when Bim_S-Bad mutants D17A and F19A were coexpressed with Bcl-2, increased cytoplasmic localization was also observed, correlating with the weaker *in vitro* affinity of these mutants for Bcl-2 (IC₅₀ ≥ 1500 nM).

We next tested the ability of ABT-737 to displace mutant BH3-only proteins from their mitochondria and ER localized pro-survival partners. We observed that mCherry-BH3 protein redistribution to the cytoplasm occurred much faster in the mutants with lower affinity for the coexpressed binding partner (Figures 4e and g) and that the observed kinetics were consistent with a model of competitive binding between ABT-737 and BH3-only affinity mutants. Additionally, we found that the potency of ABT-737 was generally higher for the lower affinity BH3-only mutant cell lines based on the displacement of the BH3-only protein at 6 h (Figures 4f and h, Table 1 and Supplementary Figures 5a–i).

Having characterized the behavior of these cell lines when treated with ABT-737, we now sought to demonstrate the concept that these lines could be used to identify lower potency chemical matter. We hypothesized that an enantiomer of ABT-737¹⁰ with ~100-fold lower potency for Bcl-x_L would cause displacement of BH3-only mutants that had sufficiently reduced affinity for Bcl-x_L. We treated Bcl-x_L cell lines expressing either Bim_S-BadBH3ΔC or Bim_S-BadBH3ΔC-D17A with the enantiomer and showed that although 100 μM of enantiomer was unable to displace the higher affinity Bim_S-BadBH3ΔC mutant, we were, however, able to determine an EC₅₀ of 611 nM for the lower affinity Bim_S-BadBH3ΔC-D17A mutant (Figure 4j and Supplementary Figures 5j and k).

Combined, these results underscore the possibility of using affinity mutants to identify compounds with desired selectivity that would otherwise be excluded by a higher stringency assay. Although such compounds may not have sufficient potency to displace wild-type BH3 proteins from the BH3-binding groove of the Bcl-2 pro-survival protein, they may nevertheless provide an appropriate starting point from which to optimize the development of inhibitors. In summary, when combined with the higher stringency wild-type Bcl-2 and BH3-only configuration of our assay, the affinity mutant approach offers the opportunity to identify and optimize diverse, specific and potent inhibitors of these protein–protein interactions that are effective in cells.

Discussion

The intrinsic apoptosis pathway is mediated by protein–protein interactions between the pro-survival and pro-apoptotic factions of the Bcl-2 super-family of proteins. Multiple experimental approaches have helped to investigate these processes, however, to date, no quantitative means of analyzing these interactions in live cells have been reported. The quantitative, high-throughput time-lapse microscopy approaches that we have described permit analysis of Bcl-2 pro-survival and BH3-only protein–protein interactions in live cells. This, along with the modular nature of our assays, make them well suited for investigating the multiplicity of these interactions.

Critically for drug screening purposes, we have illustrated the suitability of our approach for high-throughput cell-based studies by demonstrating the capability to screen hundreds of

conditions within a single experiment (Figure 4i). Furthermore, our work with affinity mutants demonstrates that we can constrain our assay to identify inhibitors within a desired range of potency.

We note that it is essential to consider how endogenous Bcl-2 family proteins may impact the behavior of our fluorescent fusion proteins and emphasize that this limitation may be overcome by incorporating BH3 mutants that are highly specific for a particular Bcl-2 family member of interest. For example, further characterization of Bim_S-Bad BH3 F19A identified it as such a relatively specific partner for Bcl-x_L. Bim_S-Bad BH3 F19A has little appreciable *in vitro* affinity for Mcl-1(3B) or Bcl-w (IC₅₀ > 10 μM in both cases) and only targets to the mitochondria in the presence of Bcl-x_L but not other Bcl-2 family members (Supplementary Figures 3d and e). This approach could be extended to other published mutants, such as the Mcl-1 specific mutant Bim_S2A.²⁹

Although we have focused our studies on demonstrating the suitability of this assay to characterize inhibitors of Bcl-2 pro-survival and BH3-only interactions in live cells, this approach can undoubtedly be extended in a number of other therapeutically relevant directions. For example, in a recent report that emphasizes the importance of understanding the potency and specificity of BH3 mimetics in a cellular and *in vivo* setting (Merino *et al.*, in revision, *Blood*), redistribution assays are used to verify that, contrary to *in vitro* binding data, Bcl-2, not Bcl-w or Bcl-x_L, is the critical target of ABT-737. Further possibilities include characterizing the mechanisms whereby BH3 mimetics such as ABT-737 combine with antimetabolic drugs³³ or other targeted agents³⁴ and investigating the mechanisms that govern a tumor's sensitivity to BH3 mimetic therapy.³⁵ Beyond the realm of therapeutic development, we expect that these assays will also be useful in characterizing the biological mechanisms that regulate interactions between pro-survival and pro-death proteins. In summary, our approach will offer many new opportunities to study how therapeutic intervention may alter the cellular mechanisms underlying apoptosis.

Materials and Methods

Molecular biology. Genes encoding fluorescent proteins were generated and cloned into the pFIT vector as previously described.¹⁶ Pro-survival constructs were cloned into the first position upstream of the pFIT IRES and pro-death constructs were cloned into the second position downstream of the IRES. tBid, Mcl-1(3B) and all ΔC mutants were generated using PCR-based mutagenesis, whereas tBidΔH6 was synthesized (DNA 2.0). Bim_S and Bim_S-BadBH3 mutants were generated by site directed mutagenesis (QuikChange Site-Directed Mutagenesis, Agilent Technologies, La Jolla, CA, USA). Details of mutations are described in Supplementary Table 1.

Cell culture, transfections and cell line engineering. All cell lines were cultured at 37 °C with 5% CO₂. HEK293T cells were grown in DMEM/F12 50:50 media with 10% fetal bovine serum (FBS) and 1 × GlutaMAX supplement (Life Technologies) and plated between 18 000–22 000 cells per well in Aurora Biotechnologies cover-slip-bottom 384-well plates (Brooks, Poway, CA, USA) 14–18 h before transfection. Transient transfections were performed using Lipofectamine 2000 Transfection Reagent (Life Technologies) according to the manufacturer's protocol for 96-well plates and scaled-down by a factor of 4 for 384-well plates. MitoTracker Deep Red dye (Life Technologies) was incubated for 1 h at a final concentration of 6 nM before live-cell imaging.

Flp-In T-REx-293 cells (Life Technologies) were cultured in DMEM/F12 50:50 media with 10% Tet-free FBS and 1 × GlutaMAX supplement. Stable T-REx-293 cell lines were generated using the FuGENE6 Transfection Reagent (Roche, Indianapolis, IN, USA) following the manufacturer's protocol. Fusion protein expression in stable T-REx-293

cell lines (plated at 18 000 cells per well) was induced with 1 μ g/ml doxycycline 14–18 h before imaging.

Compound treatment of live cells. For compound treatment of the stable T-REx-293 cell lines, cells were switched to serum-free, phenol red-free media before imaging and 2 \times concentration compounds or DMSO control were diluted in the same media and added to an equal well volume after two frames of acquisition for time-lapse studies.

Immunofluorescence. The following primary antibodies were used at the manufacturer's suggested concentrations: anti-Mcl-1 (BD Biosciences, San Diego, CA, USA, #554103), Bcl-2 (Santa Cruz Biotechnology, Santa Cruz, CA, USA, SC-7382), Bcl-x_L (Cell Signaling, Danvers, MA, USA, #2764S), Bcl-w (Santa Cruz Biotechnology, SC-130701), A1 (Santa Cruz Biotechnology, SC-6068), Noxa (Novus Biological, Littleton, CO, USA, NB600-1159), Bad (BD Biosciences, #610391), Bim_S (Cell Signaling, #2819), Puma (Abcam, Cambridge, MA, ab9643), Bid (Santa Cruz Biotechnology, SC-6538), followed by Alexa Fluor secondary antibodies used at 1 : 2000 (Life Technologies). MitoTracker Deep Red dye (Life Technologies) was incubated at 300 nM in live cells for 30 min before fixation.

Microscopy. All cells were imaged using a Nikon Ti-perfect focus inverted microscope with an A1R resonant spectral confocal system at 37 °C with 5% CO₂. High-resolution transient transfections, immunofluorescence and stable cell line images in 384-well plates were acquired with a CFI Plan Fluor \times 40 or \times 60 oil immersion objective (NA: 1.25, Nikon) as described previously.¹⁶ Low-resolution transient transfections, (Figure 3) and time-lapse compound dose treatment images were acquired with a CFI Plan Apo VC \times 20 dry objective (NA: 0.75, Nikon).

Image, data and statistical analysis. Custom image analysis programs were written in MATLAB software (MathWorks, Natick, MA, USA) (see Supplementary Note).

We noted that MitoTracker dye stains the mitochondria strongly, the cytoplasm weakly and does not stain the nucleus (Figure 1c). We used these differential staining intensities to automatically segment these three compartments (Figure 1d; Mito masking). For transiently transfected cells, intensity thresholding of the fluorescent protein signal combined with the previously defined cytoplasm mask was used to identify cells within a defined range of expression levels (Figure 1d; transfection mask). The degree of mitochondrial targeting was calculated by measuring the fluorescent protein intensity within the mitochondrial and cytoplasm masks. The resulting mitochondrial targeting ratio (mitochondria intensity/cytoplasm intensity) has an expected value of 1 for no mitochondrial targeting and elevated values for proteins that target partially to the mitochondria (e.g., Figure 1e). For transient transfections, 2–3 fields were imaged per well, for replicates of two wells for a total of 400 cells per condition. Experiments were performed at least twice.

For compound analysis, numerical data generated from image analysis in MATLAB was first normalized to values at time zero. The normalized DMSO values were averaged and then subtracted from values of the compound treatment at the appropriate time point. These normalized values were then plotted and fitted using Prism (GraphPad Software, La Jolla, CA, USA). Endpoint compound dose experiments were fitted with a variable slope sigmoid curve and time-lapse compound dose experiments were fitted to a single exponential decay curve. All error bars represent standard error and *P*-values were calculated using a Student's *t*-test.

Binding assays. The IC₅₀ values of BH3 peptides binding to pro-survival proteins were measured by surface plasmon resonance using solution competition assays performed on a Biacore 3000 as previously described.¹² Briefly, pro-survival proteins were incubated at a final concentration of 10 nM with varying concentrations of synthetic peptide for 2 h in running buffer (10 mM Hepes, 150 mM NaCl, 3.4 mM EDTA, 0.005% (v/v) Tween-20, pH 7.2) before injection onto a CM5 sensor chip on which either a wild-type BimBH3 peptide or an inert BimBH3 mutant peptide was immobilized. The specific binding of the pro-survival protein to the surface of the chip in the presence and absence of peptides was quantified by subtracting the signal from the inert BimBH3 mutant channel from that obtained on the wild-type BimBH3 channel. The ability of the peptides to prevent protein binding to immobilized BimBH3 was expressed as the IC₅₀, calculated by nonlinear curve-fitting of the data using KaleidaGraph (Synergy Software, Reading, PA, USA).

Conflict of Interest

CW, DJA and MJCL are employed at Genentech Inc., a for profit institution. WDF and EFL declare no conflict of interest.

Acknowledgements. We would like to acknowledge Lisa Belmont, Jenni Durieux, Wayne Fairbrother, John Flygare, David Huang, Peter Jackson, Deepak Sampath, Jeff Settleman, David Stokoe and Ingrid Wertz for critical reading of the manuscript and insightful comments on this work. We also thank Abbott Laboratories for providing ABT-737 and ABT-737 enantiomer compounds. EFL is supported by the Leukaemia Foundation of Australia (Phillip Desbrow Post Doctoral Fellowship) and WDF by an NHMRC Project Grant (#1008329).

Author contributions

CW, DJA and MJCL conceived the project, designed the studies, interpreted data and wrote the manuscript. CW and DJA conducted experiments and analyzed the data. EFL and WDF generated and conducted biochemical characterization of the BH3-only affinity mutants.

- Chipuk JE, Moldoveanu T, Llambi F, Parsons MJ, Green DR. The BCL-2 family reunion. *Mol Cell* 2010; **37**: 299–310.
- Youle RJ, Strasser A. The BCL-2 protein family: opposing activities that mediate cell death. *Nat Rev Mol Cell Biol* 2008; **9**: 47–59.
- Bossy-Wetzel E, Newmeyer DD, Green DR. Mitochondrial cytochrome c release in apoptosis occurs upstream of DEVD-specific caspase activation and independently of mitochondrial transmembrane depolarization. *EMBO J* 1998; **17**: 37–49.
- Tait SWG, Green DR. Mitochondria and cell death: outer membrane permeabilization and beyond. *Nat Rev Mol Cell Biol* 2010.
- Kelly PN, Strasser A. The role of Bcl-2 and its pro-survival relatives in tumourigenesis and cancer therapy. *Cell Death Differ* 2011; **18**: 1414–1424.
- Adams JM, Cory S. The Bcl-2 apoptotic switch in cancer development and therapy. *Oncogene* 2007; **26**: 1324–1337.
- Fesik SW. Promoting apoptosis as a strategy for cancer drug discovery. *Nat Rev Cancer* 2005; **5**: 876–885.
- Lessene G, Czabotar PE, Colman PM. BCL-2 family antagonists for cancer therapy. *Nat Rev Drug Discov* 2008; **7**: 989–1000.
- Kang MH, Reynolds CP. Bcl-2 inhibitors: targeting mitochondrial apoptotic pathways in cancer therapy. *Clin Cancer Res* 2009; **15**: 1126–1132.
- Oltersdorf T, Elmore SW, Shoemaker AR, Armstrong RC, Augeri DJ, Belli BA et al. An inhibitor of Bcl-2 family proteins induces regression of solid tumours. *Nature* 2005; **435**: 677–681.
- Zhai D, Jin C, Shiau C-W, Kitada S, Satterthwait AC, Reed JC. Gambogic acid is an antagonist of antiapoptotic Bcl-2 family proteins. *Mol Cancer Ther* 2008; **7**: 1639–1646.
- Chen L, Willis SN, Wei A, Smith BJ, Fletcher JL, Hinds MG et al. Differential targeting of prosurvival Bcl-2 proteins by their BH3-only ligands allows complementary apoptotic function. *Mol Cell* 2005; **17**: 393–403.
- Certo M, Del Gaizo Moore V, Nishino M, Wei G, Korsmeyer S, Armstrong SA et al. Mitochondria primed by death signals determine cellular addiction to antiapoptotic BCL-2 family members. *Cancer Cell* 2006; **9**: 351–365.
- Ku B, Liang C, Jung JU, Oh BH. Evidence that inhibition of BAX activation by BCL-2 involves its tight and preferential interaction with the BH3 domain of BAX. *Cell Res* 2011; **21**: 627–641.
- Leber B, Lin J, Andrews DW. Still embedded together binding to membranes regulates Bcl-2 protein interactions. *Oncogene* 2010; **29**: 5221–5230.
- Anderson DJ, Durieux JK, Song K, Alvarado R, Jackson PK, Hatzivassiliou G et al. Live-cell microscopy reveals small molecule inhibitor effects on MAPK pathway dynamics. *PLoS ONE* 2011; **6**: e22607.
- Nguyen M, Millar DG, Yong VW, Korsmeyer SJ, Shore GC. Targeting of Bcl-2 to the mitochondrial outer membrane by a COOH-terminal signal anchor sequence. *J Biol Chem* 1993; **268**: 25265–25268.
- Krajewski S, Tanaka S, Takayama S, Schibler MJ, Fenton W, Reed JC. Investigation of the subcellular distribution of the bcl-2 oncoprotein: residence in the nuclear envelope, endoplasmic reticulum, and outer mitochondrial membranes. *Cancer Res* 1993; **53**: 4701–4714.
- Akao Y, Otsuki Y, Kataoka S, Ito Y, Tsujimoto Y. Multiple subcellular localization of bcl-2: detection in nuclear outer membrane, endoplasmic reticulum membrane, and mitochondrial membranes. *Cancer Res* 1994; **54**: 2468–2471.
- Germain M, Duronio V. The N terminus of the anti-apoptotic BCL-2 homologue MCL-1 regulates its localization and function. *J Biol Chem* 2007; **282**: 32233–32242.
- Kaufmann T, Schlipf S, Sanz J, Neubert K, Stein R, Borner C. Characterization of the signal that directs Bcl-x(L), but not Bcl-2, to the mitochondrial outer membrane. *J Cell Biol* 2003; **160**: 53–64.
- Weber A, Paschen SA, Heger K, Wilfling F, Frankenberg T, Bauerschmitt H et al. BimS-induced apoptosis requires mitochondrial localization but not interaction with anti-apoptotic Bcl-2 proteins. *J Cell Biol* 2007; **177**: 625–636.
- Nakano K, Voutsden KH. PUMA, a novel proapoptotic gene, is induced by p53. *Mol Cell* 2001; **7**: 683–694.
- Oda E, Ohki R, Murasawa H, Nemoto J, Shibue T, Yamashita T et al. Noxa, a BH3-only member of the Bcl-2 family and candidate mediator of p53-induced apoptosis. *Science* 2000; **288**: 1053–1058.

25. Seo Y-W, Shin JN, Ko KH, Cha JH, Park JY, Lee BR *et al*. The molecular mechanism of Noxa-induced mitochondrial dysfunction in p53-mediated cell death. *J Biol Chem* 2003; **278**: 48292–48299.
26. Li H, Zhu H, Xu CJ, Yuan J. Cleavage of BID by caspase 8 mediates the mitochondrial damage in the Fas pathway of apoptosis. *Cell* 1998; **94**: 491–501.
27. Luo X, Budihardjo I, Zou H, Slaughter C, Wang X. Bid, a Bcl2 interacting protein, mediates cytochrome c release from mitochondria in response to activation of cell surface death receptors. *Cell* 1998; **94**: 481–490.
28. Gonzalez F, Pariselli F, Jalmar O, Dupaigne P, Sureau F, Dellinger M *et al*. Mechanistic issues of the interaction of the hairpin-forming domain of tBid with mitochondrial cardiolipin. *PLoS ONE* 2010; **5**: e9342.
29. Lee EF, Czabotar PE, van Delft MF, Michalak EM, Boyle MJ, Willis SN *et al*. A novel BH3 ligand that selectively targets Mcl-1 reveals that apoptosis can proceed without Mcl-1 degradation. *J Cell Biol* 2008; **180**: 341–355.
30. Albershardt TC, Salerni BL, Soderquist RS, Bates DJP, Pletnev AA, Kisselev AF *et al*. Multiple BH3 mimetics antagonize antiapoptotic MCL1 protein by inducing the endoplasmic reticulum stress response and up-regulating BH3-only protein NOXA. *J Biol Chem* 2011; **286**: 24882–24895.
31. Sattler M, Liang H, Nettesheim D, Meadows RP, Harlan JE, Eberstadt M *et al*. Structure of Bcl-xL-Bak peptide complex: recognition between regulators of apoptosis. *Science* 1997; **275**: 983–986.
32. Lee EF, Czabotar PE, Smith BJ, Deshayes K, Zobel K, Colman PM *et al*. Crystal structure of ABT-737 complexed with Bcl-xL: implications for selectivity of antagonists of the Bcl-2 family. *Cell Death Differ* 2007; **14**: 1711–1713.
33. Shi J, Zhou Y, Huang H-C, Mitchison TJ. Navitoclax (ABT-263) Accelerates Apoptosis during Drug-Induced Mitotic Arrest by Antagonizing Bcl-xL. *Cancer Res* 2011; **71**: 4518–4526.
34. Hikita H, Takehara T, Shimizu S, Kodama T, Shigekawa M, Iwase K *et al*. The Bcl-xL inhibitor, ABT-737, efficiently induces apoptosis and suppresses growth of hepatoma cells in combination with sorafenib. *Hepatology* 2010; **52**: 1310–1321.
35. Harrison LR, Micha D, Brandenburg M, Simpson KL, Morrow CJ, Denny O *et al*. Hypoxic human cancer cells are sensitized to BH-3 mimetic-induced apoptosis via downregulation of the Bcl-2 protein Mcl-1. *J Clin Invest* 2011; **121**: 1075–1087.



Cell Death and Disease is an open-access journal published by **Nature Publishing Group**. This work is licensed under the **Creative Commons Attribution-NonCommercial-No Derivative Works 3.0 Unported License**. To view a copy of this license, visit <http://creativecommons.org/licenses/by-nc-nd/3.0/>

Supplementary Information accompanies the paper on Cell Death and Disease website (<http://www.nature.com/cddis>)